Performance of Optimized MultiChannel Image Noise Filters

Mark Gorzynski
Hewlett-Packard Company
Corvallis, Oregon

Abstract

This paper describes the use of custom Wiener Spectrum filters for evaluation of image noise. The method involves dividing the spectrum into radial and angular bands and computing volumes for each band. The band volumes are then compared to visual data to determine desired model form and band weightings. If desired, the resulting models automatically account for acquisition and visual transfer functions. An example of model optimization for Ink Jet mottle and banding rejection is described. The optimized model predicts visual quality results.Introduction

Introduction

During design phases, ink jet printers produce images that suffer from a variety of spatial print defects. These defects include grain, mottle, halftone texture, dot and mechanism induced artifacts, banding and pen-matrix induced texture. Engineers need to measure the magnitude of defects to help debug systems, set specifications and establish tolerances on components.

The accessibility of high quality desktop scanners and digital cameras combined with commercial image processing software makes implementation and experimentation with image noise analysis easy for day-to-day use in industry. Complex models can be easily implemented and put into immediate use evaluating hundreds of samples. When measuring an ever-changing variety of noise defects, workers in our lab have claimed poor success using any one single noise measure for all. In this environment, a flexible approach has been more useful.

Authors have reviewed a variety of noise measures that have been reported over the years.[1,2,10,11,12] Popular methods include VTF-weighted Wiener Spectra[3,4,5,6], and more complex multiple channel methods.[2,11,12] The variety of published methods provide a framework for flexible model development for the applied worker. Johannson and Nystrom have reported successful use of filtered Wiener Spectra for noise analysis in the Graphic Arts[7,8]. Rather than a single VTF function, they optimize sets of filters as

needed. In Ink Jet applications, we also have found that Wiener Spectrum analysis with single or multiple custom filters can provide useful noise metrics.

A Generic Noise Model Framework

Many components have been added to noise models over the years to account for visual and acquisition system properties. For many applications, we have found a simple class of Wiener Spectrum models with an abbreviated set of components satisfactory. There are many possibilities, for example, equation (1).

$$DNS = \beta_0 + \beta_1 \left[\sum_k \left(w_k \sum_i \sum_j \sqrt{WS_R(i,j)} F_k(i,j) \right) \right]^{\beta_3} \quad (1)$$

Where WSR(i,j) is the reflectance Wiener Spectrum for an image region with frequency sampling i,j, Fk(i,j) represents a set of filters at the same sampling rate and wk are a set of weights corresponding to the k filters.

The reflectance weighting of the Wiener Spectrum depends on the application. In most cases, simple photopic weighting is used for an achromatic response. Cone or achromatic-chromatic weightings could also be used[2,13].

This example metric is a weighted sum of the volumes under each filter. If the filters Fk(i,j) add together to form a VTF, equation (2) is equivalent to models such as one propose by Shaw and McGuire[3,4,5,6] except for the added constants. Shaw and McGuire's digital noise scale (DNS) is expressed in equation (2).

$$DNS = \sqrt{WS_R(u,v)VTF^2(u,v)} \quad (2)$$

Where WS_R represents the Wiener Spectrum in reflectance units and VTF denotes a visual transfer function as in McGuire and Shaw (1997).

The constants of (1) add some simple rescaling and nonlinearity capability to account for a perceptual quality or visual noise scaling results. There are many other possibilities for combining the k filtered spectra to account for other factors such as masking or adaptation.

Using a filter set rather than a VTF (CSF) provides several advantages. First there is the mentioned flexibility in modeling. Second, the spectral weighting can be adjusted to fit the visual results of a particular experiment creating a custom VTF. As confidence is gained in the weighting, the new VTF could be standardized for longer-term use. Finally, if the weights are optimized without correcting the Wiener Spectrum for acquisition system transfer function, their values will include this correction. While this is advantageous for simplicity, combining acquisition transfer function correction with VTF makes the model non-robust for optical changes. If robustness is required, a traditional correction factor can be included as a separately characterized function before optimization of weights and constants to visual results.

Wiener Spectrum Estimation

Often, fast image processing cycle times are required making it advantageous to use the squared magnitude of the discrete Fourier transform as an estimate of the Wiener Spectrum. In these cases, signal averaging is used to help reduce the large variance associated with this type of estimate. We have used Welch-type averaging[9] with a Bartlett data window with some success. There are quite a few other issues such as image window size, FFT window size and placement and image sampling rate. The band pass characteristics of the filters needed for visual modeling yield practical limits for sampling rates. 600spi has be more than enough for most visual applications but higher rates may be needed for analytic inspection of microstructure or hardware signals.

Choice of Filters

On our desktop systems, we have implemented families of standard filter types for general use. Rectangular and Gaussian filters are commonly used. For example, the set of Gaussian bandpass functions shown in figure (1) can be selected to create a set of annular band pass filters as shown in figure (2). These can be combined with directional filters as in figure (3) to create a set of notch filters aligned along an axis as in figure (4). These filters are typical of ones used to optimize a response function for banding.

Example: Ink Jet Mottle Insensitive to Banding

Consider a case where a team wanted to optimize an ink system for minimal plain paper mottle. The team requested an automated optical system that correlated to print quality degradations due to mottle. They wanted to use this system to evaluate their ink treatments. Filling these needs required a) creation of a scale of visual quality and b) implementation of an algorithm for mottle on one of several available image analysis systems.

The experimenters required a measure relating to print *quality* rather than perceived amount of mottle. This is a common requirement arising from the need to express treatment results in terms of progress to program quality goals. For visual scaling, a simplified print was created
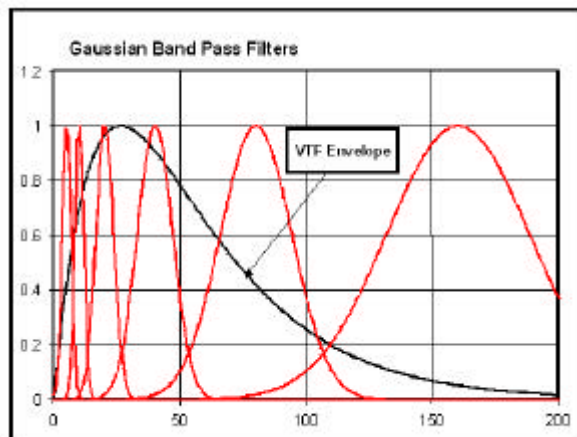

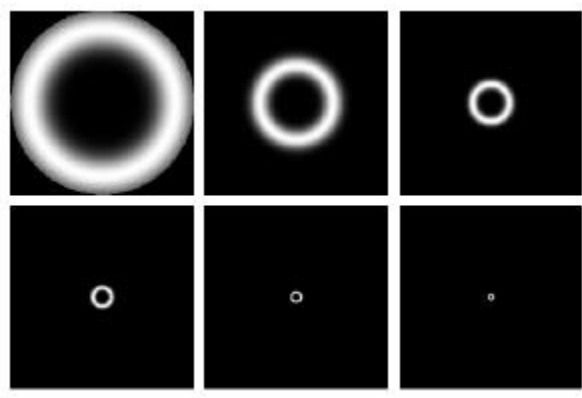*Figure 1. Example Gaussian band pass filters.*

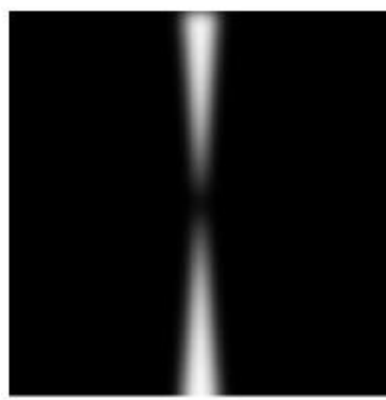*Figure 2. Image of Gaussian band pass filters.*
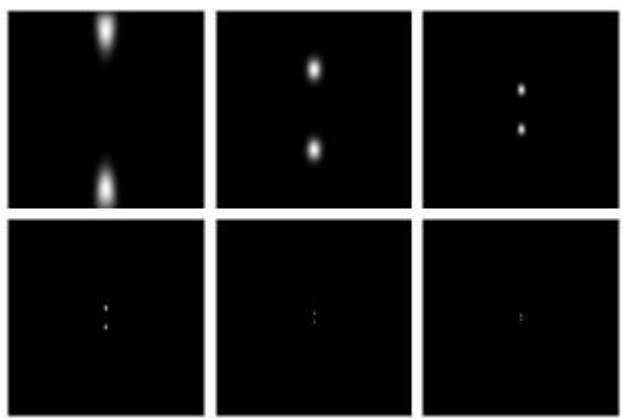

Figure 3. Example of directionally sensitive filter.

Figure 4. A set of filters optimized for banding measurement.

Figure 5. Results of model optimization for mottle data.

consisting of a "palette" of colored 1-inch squares. These patches were evaluated for "quality" using a rating-scale method and a pool of observers that rated color graphics prints for quality on a weekly basis.

The necessity to predict quality led us to define a two-stage model to cover both mottle noise magnitude and quality nonlinearity. The model shown in equation (1) includes a power function that is sufficient for quality nonlinearities of moderate scale.

To determine the type of filter optimization and combination required, the Wiener Spectra of the test patches were compared to determine what signals were present. Tests showed a mottle signal at low frequencies, banding signals at a range of frequencies aligned along the vertical axis and higher frequency halftone signals. Halftone noise was color dependent. Banding was more random depending on a number of mechanism and pen factors.

Because banding was not constant within one color of patch, visual quality scores with and without banding could be compared for a single ink treatment. As expected, banding decreased quality. It was concluded that at constant levels of mottle, quality is degraded by additional banding and halftone noise. Alternatively, at constant levels of halftone, or banding, increases in mottle decrease quality. The goal was restated to produce a system that evaluates mottle in a fashion independent of banding and halftone noise. To achieve this, a set of filters was designed to remove spatial frequency signals for halftone and banding leaving signals from mottle.

Since mottle is not directionally sensitive, its spectrum could be evaluated without the vertical axis containing banding data. The high frequency characteristics of halftone could also be removed without destroying the lower frequency mottle signal. A set of low frequency band pass filters was prepared with notched out vertical axes. These were optimized for the noise model shown in equation (3).
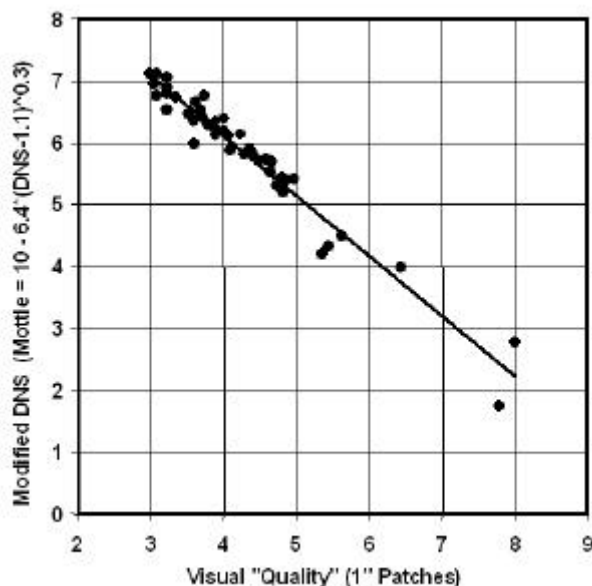
The constants of equation (3) are the results obtained from a nonlinear optimization of equation (1) to the mottle quality data. The model results are plotted against the visual quality ratings in figure 5 for an image test set free of banding. If good correlation is achieved for these samples, at least the mottle portion of the model is working. Finally, samples with and without banding from the same ink treatment were measured. These were scored similarly by the new model indicating it was relatively insenstive to banding.

$$M = 10 + 6.4(DNS + 1.1)^{0.3} \qquad (3)$$

Conclusion

A generic framework for optimizing filtered Wiener Spectrum models to visual noise data is used successfully in ink jet R&D to address complex defect measurement. The large set of image and signal processing tools available for spectral analysis make this a very flexible method.

References

1. R. E. Jacobson, *J. Photogr. Sci*. **43**, 7 (1995).
2. S. N. Pattaniak, J. A. Ferwerda, M. D. Fairchild, and D. P. Greenberg, *Procs SIGGRAPH 98*, 287 (1998).
3. R. Shaw, *Procs NIP 12*, 162 (1996).
4. R. Shaw, *Procs NIP 13*, 562 (1997).

5. R. Shaw, *Procs NIP 14*, 582 (1998).
6. M. McGuire and R. Shaw, *Procs NIP 13*, 566 (1997).
7. P. Johansson, *Procs 22nd Research Conference of the International Association of Research Institutes for the Graphic Arts Industry*, *Munich*, 403 (1993).
8. S. Nystrom and P. Johansson, *Presentation at the PTS Image Analysis Symposium, Munich*, (1998).
9. P. D. Welch, *IEEE Trans. Audio electroacoust*. 70 (1967).
10. K. R. Boff and J. E. Lincoln, *Engineering Data Compendium: Human Perception and Performance.* AAMRL 310, 1988.
11. S. Daly, *Procs SPIE* 1616, 2 (1992).
12. J. E. Farrell, X. Zhang, C. van den Branden Lambrecht and D. Silverstein, *Procs COMPCON*, (1997).
13. X. M. Zhang and B. A. Wandell, *SID 96 Digest*, 731, (1996).